Extended Abstracts of the 2018 International Conference on Solid State Devices and Materials, Tokyo, 2018, pp745-746

Determining the Carrier Mobility in Single InAs Nanowires from Magnetotransport Measurements

Patrick Uredat[1, 2], Ryutaro Kodaira[3], Ryoma Horiguchi[3], Shinjiro Hara[3], Peter J. Klar[1, 2], and Matthias T. Elm[1, 2, 4]

[1] Center for Materials Research,
Justus Liebig University, 35392 Giessen, Germany
Phone: +49-641-9933147 E-mail: patrick.uredat@physik.uni-giessen.de
[2] Institute of Experimental Physics I,
Justus Liebig University, 35392 Giessen, Germany
[3] Research Center for Integrated Quantum Electronics,
Hokkaido University, Sapporo 060-8628, Japan
[4] Institute of Physical Chemistry,
Justus Liebig University, 35392 Giessen, Germany

Abstract

Here, we present magnetotransport properties of single InAs nanowires grown by selective-area metal-organic vapor-phase epitaxy. The semiconducting InAs nanowires exhibit quantum interference effects as well as a large positive magnetoresistance effect. Angle-dependent transport measurements reveal additional boundary scattering due to the confined transport channel offering a possibility of determination both the carrier concentration and the electron mobility.

1. Introduction

Semiconducting nanowires increasingly attract attention as building blocks for future nanoscaled electronic or optoelectronic devices, such as field-effect transistors (FET), gas sensors or light-emitting diodes. Moreover, nanowires are an ideal model system to study the electronic transport trough confined systems due to their spatial dimension of a few nanometers. In particular, InAs nanowires are intriguing because of their low effective masses and high electron mobilities together with a strong spin-orbit coupling and a large g-factor. These properties make InAs nanowires interesting not only for high-speed electronics but also for future spintronic devices, such as spin FET [1, 2].

2. General Instructions

InAs nanowires were grown by selective-area metal-organic vapor-phase epitaxy (MOVPE). The fabrication process of the nanowires comprises several steps. First, an amorphous SiO_2-layer of about 30 nm is deposited on a (111)B-GaAs substrate. This layer is then structured by electron beam lithography followed by reactive ion etching to form circular pinholes in the SiO_2 layer with diameters of about 80 to 90 nm and a pitch of about 1 μm between the openings. In these openings the InAs nanowires start growing during MOVPE. We supplied $(CH_3)_3In$ and 20%-AsH_3 diluted in H_2 as organometallic and hydride sources, respectively. The growth temperature T_g and the growth time t_g were 560°C and 30 min, respectively. Structural characterization was carried out by transmission electron miscopy studies. Cross-sectional lattice images reveal zinc-blende type InAs nanowires with high structural quality. The growth direction of the nanowires is parallel to the <111>B direction of the substrate. After the growth the InAs nanowires were detached from the substrate by ultrasonic vibration in isopropanol solution and then deposited on a SiO_2/Si substrate. In order to obtain ohmic contacts the native oxide layer was removed by Ar milling at 30 W for 60 sec. Afterwards, electronic contacts of Ti/Au 25 nm/165 nm were structured by electron-beam lithography and electron beam evaporation.

3. Results and Discussion

The transport properties of single InAs nanowires have been studied using a He-4 flow cryostat with a superconducting magnet supplying external magnetic fields up to 10 T. The temperature-dependence of the InAs nanowire resistivity was investigated in two-probe geometry in a temperature range between 1.7 K and 280 K. The resistivity exhibits a semiconducting behavior in the range between room temperature and 10 K. For temperatures below 10 K the resistivity decreased slightly with decreasing temperature owing to a metallic transport process.

Magnetotransport measurements have been conducted for various temperatures. A large positive ordinary magnetoresistance effect up to 150% was observed for temperatures between 280 K and 120 K. In addition, weak localization as well as universal conductance fluctuation arise at low temperatures. Beyond that, the magnetotransport measurements have been performed for different orientations of the nanowire to the applied magnetic field. Exemplary for different temperatures, the magnetoresistance at 120 K is shown in Fig. 1 as a function of the squared magnetic field for a perpendicular and parallel orientation.

As the positive ordinary magnetoresistance effect is proportional to the squared magnetic field, the magnetoresistance in Fig. 1 should give a straight line. This applies for the parallel but not for the perpendicular orientation. In the

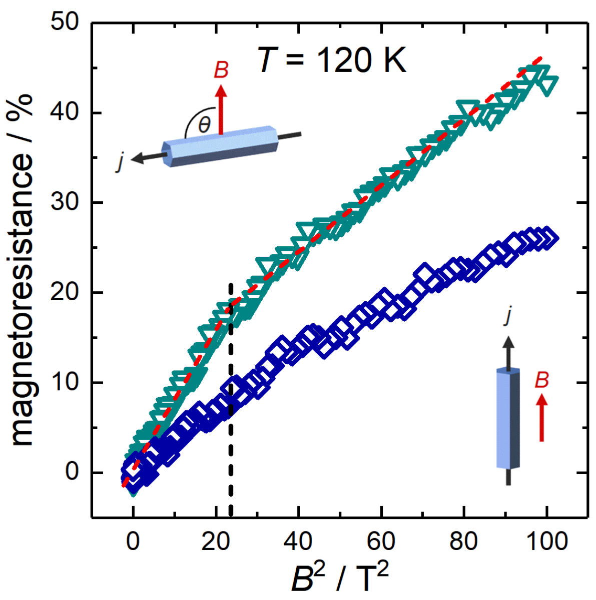

Fig. 1: Magnetoresistance as a function of the squared magnetic field for perpendicular and parallel orientation of the nanowire to the magnetic field.

perpendicular orientation a kink occurs at a squared magnetic field of $B^2 \approx 22\ \mathrm{T}^2$. This kink can be explained by classical boundary scattering in a diffusive transport regime. As explained by Beenakker and van Houten [3], the magnetic field forces the electrons on circular orbits. When the carriers reach the boundary of the nanowire, additional backscattering occurs, which results in a higher resistivity of the nanowire. The radius r_{circ} of these orbits is proportional to the mobility μ and inversely proportional to the applied magnetic field B and the carrier concentration n:

$$r_{\mathrm{circ}} = \frac{v}{\omega} = \frac{m}{e}\frac{\mu}{B}\frac{V_0}{L} = \frac{m}{e^2}\frac{j}{nB}, \qquad (1)$$

where $\mathcal{E} = V_0/L$ and j are the applied electric field and the current density, respectively.

The backscattering contribution reaches its maximum when the orbit radius is twice the diameter W of the nanowire. As the radius r_{circ} decreases by further increasing the magnetic field, boundary scattering is reduced leading to a change in the slope of the magnetoresistance and thus to the kink observed in Fig. 1 for $B \perp$ nanowire. This effect does not occur in parallel orientation as the electrons are not deflected towards the boundary of the nanowire by the external magnetic field.

As backscattering is maximal for $r_{\mathrm{circ}} = 2W$ the carrier concentration in the nanowire was estimated with eq. (1) from the magnetic field value where the kink occurs. For m the effective electron mass in InAs of $0.023\ m_0$ was used. As the kink shifts to smaller magnetic fields with increasing temperature, carrier concentrations were obtained in the temperature range from 120 to 160 K. The temperature dependence of the carrier concentration are plotted in Fig. 2 in an Arrhenius representation yielding an activation energy of about 37

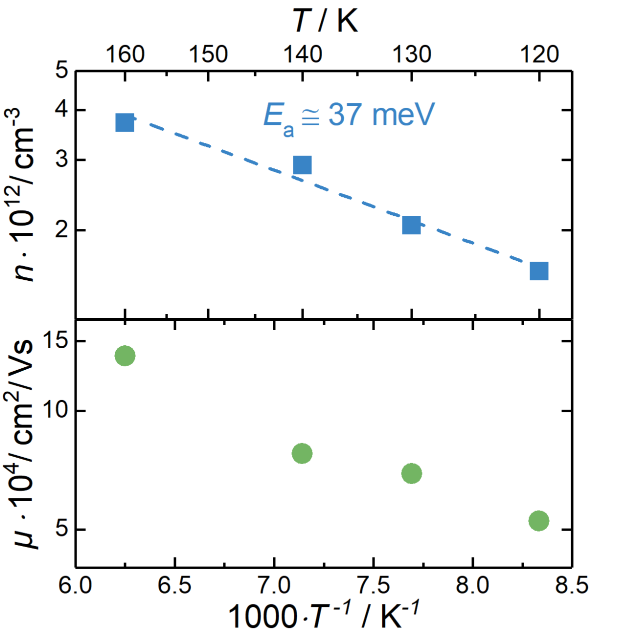

Fig. 2: Determined values for the carrier concentration and electron mobility as a function of inverse temperature for the unintentionally doped InAs nanowire.

meV. The absolute values for the carrier concentration in the conduction band vary between $1 - 4 \times 10^{12}\ \mathrm{cm}^{-3}$ which is approximately one order of magnitude higher than the intrinsic carrier concentration in InAs.

Furthermore, the electron mobility was calculated with eq. (1). For the unintentionally doped InAs nanowires electron mobilities of about $5 \times 10^4\ \mathrm{cm}^2\mathrm{V}^{-1}\mathrm{s}^{-1}$ to $1.5 \times 10^5\ \mathrm{cm}^2\mathrm{V}^{-1}\mathrm{s}^{-1}$ have been obtained, which is comparable to values reported in literature [4, 5].

4. Conclusions

Magnetotransport measurements of single InAs nanowires grown by selective-area MOVPE reveal additional boundary scattering due to the confined transport channel. As the contribution of the additional boundary scattering depends on the strength of the applied magnetic field it can be used to determine the electron mobility and the carrier concentration for known diameter of the nanowire investigated. This may open a new approach for determining the mobility and carrier concentration in nanostructures.

References

[1] M. T. Elm and S. Hara, Adv. Mater. **26**, (2014) 8079.

[2] T. Tanaka, K. Tomioka, S. Hara, J. Motohisa, E. Sano, and T. Fukui, Appl. Phys. Express **3**, (2010) 025003.

[3] C. W. J. Beenakker and H. van Houten, Solid State Phys. **44**, (1991) 1.

[4] N. Gupta, Y. Song, G. W. Holloway, U. Sinha, C. M. Haapamaki, R. R. LaPierre, and J. Baugh, Nanotechnology **24**, (2013) 225202.

[5] M. Scheffler, S. Nadj-Perge, L. P. Kouwenhoven, M. T. Borgström, and E. P. A. M. Bakkers, J. App. Phys. **106**, (2009) 124303.